Title

Long-Term Ligature-Induced Periodontitis Exacerbates Development of Bisphosphonate-Related Osteonecrosis of the Jaw in Mice

Journal

Journal of Bone and Mineral Research, 37(7)

ISSN

0884-0431

Authors

Williams, Drake Winslow
Ho, Katie
Lenon, Allison
et al.

Publication Date

2022-07-01

DOI

10.1002/jbmr.4614

Peer reviewed

HHS Public Access

Author manuscript

J Bone Miner Res. Author manuscript; available in PMC 2022 August 18.

Published in final edited form as:

J Bone Miner Res. 2022 July ; 37(7): 1400–1410. doi:10.1002/jbmr.4614.

Long-term ligature-induced periodontitis exacerbates bisphosphonate-associated osteonecrosis development

Drake Winslow Williams[1,2,*,**], **Katie Ho**[1], **Allison Lenon**[1], **Sol Kim**[1,2], **Terresa Kim**[1], **Yousang Gwack**[3], **Reuben H. Kim**[1,2,4,*]

[1]The Shapiro Family Laboratory of Viral Oncology and Aging Research, Los Angeles, CA, 90095, USA

[2]Section of Restorative Dentistry, UCLA School of Dentistry, Los Angeles, CA, 90095, USA

[3]Department of Physiology, David Geffen School of Medicine, University of California, Los Angeles, CA, 90095, USA

[4]UCLA Jonsson Comprehensive Cancer Center, University of California, Los Angeles, Los Angeles CA 90095

Abstract

Bisphosphonate-related osteonecrosis of the jaw (BRONJ) is a detrimental intraoral lesion that occurs in patients with long-term or high-dose use of anti-resorptive agents such as bisphosphonates. Tooth extraction is a known risk factor for BRONJ, and such intervention is often performed to eliminate existing pathological inflammatory conditions. Previously, we determined that ligature-induced periodontitis (LIP) is a risk factor for the development of osteonecrosis in mice, but it remains unclear whether the chronicity of LIP followed by extraction influences osteonecrosis development. In this study, we assess the effect of short- and long-term LIP (ligature placed for 3 [S-LIP] or 10 [L-LIP] weeks, respectively) on osteonecrosis development in mice receiving 250μg/kg/wk zoledronic acid (ZOL). When compared to S-LIP, L-LIP caused 70% ($p \leq 0.0014$) more bone loss without altering microbe composition. In the presence of ZOL, bone loss mediated by LIP was prevented and bone necrosis was induced. When the ligated tooth was extracted, histologic hallmarks of osteonecrosis including empty lacunae and necrotic bone were increased by 88% ($p=0.0374$) and 114% ($p=0.0457$), respectively, in L-LIP compared to S-LIP. We also observed significant increases in serum PF4 and MIP-1γ in mice that received ZOL treatment and had tooth extractions compared to controls, which may be systemic markers of inflammation-associated osteonecrosis development. Additionally, CD3+ T cells were identified as the major immune population in both health and disease, and we observed a 116% ($p=0.0402$) increase in CD3+IL23R+ T cells in L-LIP compared to S-LIP lesions following extraction. Taken together, our study reveals that extracting a periodontally compromised tooth increases the formation of necrotic bone compared to extracting a periodontally healthy tooth

*Correspondence to: Drake Winslow Williams, DDS, PhD drakewilliams@gmail.com; Reuben H. Kim, DDS, PhD, UCLA School of Dentistry, Center for the Health Sciences, Room 43-091, 10833 Le Conte Ave, Los Angeles, CA90095. Phone: (310) 825-7312. Fax: (310) 825-2536. rkim@dentistry.ucla.edu.

**Present address: Oral Immunity and Inflammation Section, National Institute of Dental and Craniofacial Research, National Institutes of Health, Bethesda, MD 20892

and that osteonecrosis may be associated with the duration of the pre-existing pathological inflammatory conditions.

Keywords

BRONJ; ligature-induced periodontitis (LIP); long-term; inflammation

INTRODUCTION

Antiresorptive therapy with bisphosphonates such as zoledronic acid (ZOL) is the current front-line therapy for bone degenerative diseases such as osteoporosis [(1)]. Additionally, bisphosphonates are becoming an increasingly important tool in reducing bone pain and skeletal related events in metastatic bone disease [(2)]. Nitrogen containing bisphosphonates including ZOL act by inhibiting post-translational prenylation of proteins critical for osteoclast function, ultimately leading to inhibition of osteoclast-mediated bone resorption [(3)].

A rare but detrimental side effect of bisphosphonates is the development of bisphosphonate-related osteonecrosis of the jaw (BRONJ), which often occurs at the site of a tooth extraction or invasive dental surgery [(4)]. The pathophysiology of BRONJ has been extensively studied since the first report in 2003 [(5)] but remains elusive to date [(6)]. Notable current hypotheses to explain BRONJ development include bone remodeling inhibition [(7)], inflammation and infection [(8,9)], angiogenesis inhibition [(10)], soft tissue toxicity [(11)], and innate or acquired immune dysfunction [(12)].

While several risk factors for BRONJ development have been reported in the literature, many reported BRONJ cases occur following the extraction of a tooth with local pathologic inflammation [(13,14)]. This clinical observation has been corroborated in several animal models of periodontal and periapical disease with concomitant antiresorptive treatment and tooth extraction [(8,9,15,16)]. These studies have established that localized periodontal inflammation is a *bona fide* risk factor for BRONJ-like lesion development in mice.

Periodontal inflammation increases necrotic bone formation compared to antiresorptive treatment alone in animal studies. However, it is not known whether the duration of periodontal inflammation influences osteonecrosis development in mice. In the following study, we investigate and compare the effect of short-term (3 weeks) and long-term (10 weeks) ligature induced periodontitis (S-LIP and L-LIP, respectively) on histologic osteonecrosis, innate and adaptive immune recruitment, and local microbiota composition.

MATERIALS AND METHODS

Animals

Eight week-old female C57BL/6J mice were purchased from the Jackson Laboratories and housed in a specific pathogen free environment with 12-hour light/dark cycle managed by the UCLA Division of Laboratory and Animal Medicine. All experimental protocols were

approved by institutional guidelines from the Chancellor's Animal Research Committee (2011-062).

Ligature-induced periodontitis mouse models

We have modified our previously established mouse model for osteonecrosis development [7] to include varying times of ligature-induced inflammation preceding the tooth extraction and healing phase. The S-LIP timepoint was selected based on a previous study [8], and the L-LIP timepoint was determined to be the maximum amount of time a ligature could be placed before bone loss led to tooth exfoliation [17].

In the first set of experiments, mice were subjected to either S-LIP or L-LIP using a 6-0 silk suture around the second maxillary molar (M2) without any anti-resorptive intervention (Supplemental Fig. 1A). A second cohort of mice were subjected to L-LIP while undergoing biweekly intravenous infusions of 0.9% NaCl (Veh) or Zoledronic Acid (ZOL; 125μg/kg; Sagent Pharmaceuticals) (Fig. 3A). A third cohort of mice underwent L-LIP and ZOL treatment followed by M2 extraction and healing for three weeks (Fig. 4A). A final cohort of mice underwent either S-LIP or L-LIP and ZOL treatment followed by M2 extraction and healing for three weeks (Supplemental Fig. 6A). The mouse equivalent dose of ZOL was based on allometric scaling [18] of the human dose for the treatment of multiple myeloma.

Micro-computed tomography and bone loss analysis

Whole maxillae were scanned with a voxel size of $10\mu m^3$ using a 1.0 mm aluminum filter at 60 kVp and 166μA (SkyScan 1275; Bruker). Other scanning parameters include rotation step of 0.4 degrees, frame averaging of 6 and random movement. Two-dimensional images were reconstructed using N Recon (Bruker) following X-Y alignment and dynamic range adjustment. Reconstructed images were saved as 16-bit TIFF images and used for bone loss analysis. Bone loss was quantified by measuring the distance between cementoenamel junction (CEJ) and the alveolar bone crest (ABC) on the palatal, mesiobuccal and distobuccal roots of M2 using CTAn (Bruker). 3-dimensional representative images were generated in CTVox (Bruker).

Histochemical staining

Histologic osteonecrosis lesions were evaluated by hematoxylin and eosin staining following decalcification and paraffin embedding as described previously without modification [7]. The number of bone-lining tartrate-resistant acid phosphatase-positive osteoclasts were determined around the M2 region with a kit according to the manufacturer's protocol (#387A-1KT, Millipore Sigma).

Immunofluorescence staining

Formalin fixed paraffin embedded tissues were rehydrated by serial dilutions of xylene and ethanol. Antigen retrieval in citrate buffer was carried out at 60°C overnight. Sections were blocked in 10% normal goat serum and incubated in primary antibody diluted in 3% serum overnight at 4°C. Primary antibodies included CD3 (#ab5690, Abcam), CD66b (#ab197678, Abcam), F4/80 (#MCA497GA, Bio-Rad), and IL23R (#ab53656, Abcam). After washing, secondary antibody diluted in 3% serum was incubated for 1 hour followed by DAPI

counterstain for 8 minutes. Slides were mounted using Prolong Gold (P36930; Thermofisher Scientific) and imaged with a confocal microscope (LSM700; Zeiss).

Multiplexed sandwich ELISA Array

Sera from S-LIP and L-LIP animals with and without ZOL treatment were assayed to determine changes in 40 different pro-inflammatory cytokines following the manufacturer's protocol (#QAM-CYT-5; RayBiotech). Glass slides were imaged by RayBiotech and raw data was extracted and analyzed in Excel and Graphpad Prism ver. 6.01.

Quantitative real-time PCR

To assess local changes in inflammatory cytokines, palatal tissues immediately adjacent to the ligated M2 were isolated and processed to obtain cDNA using qScript cDNA SuperMix following manufacturer's protocol (#101414-108; VWR). Gene expression was assessed using PowerUp SYBR Green Master Mix (#100029284; Applied Biosystems) in a QuantStudio 3 Real-Time PCR System (Applied Biosystems). Fold differences between samples were calculated with the ΔΔCt method using 18S as the housekeeping gene. Primer sequences can be found in Supplemental Table 1.

16S Sequencing

Bacterial DNA was extracted from fecal and oral samples, sequenced and analyzed as described previously [19].

Statistical Analysis

All quantitative data are shown as points in boxplots. For all figures, statistical tests and results were performed with GraphPad Prism 8 and are noted on the figure itself and in the corresponding figure legend.

RESULTS

Long-term ligature placement exacerbates bone loss and pro-inflammatory cytokine expression

To determine the effect of prolonged ligature treatment in mice, we compared local consequences of S-LIP and L-LIP (Supplemental Fig. 1A). Photographic examination revealed an increase in blanched areas surrounding L-LIP sites compared to S-LIP and no-ligature control (NLC) sites (Supplemental Fig. 1B). μCT analysis showed a marked increase in the area of bone resorption at L-LIP sites compared to S-LIP (Supplemental Fig. 1C). As previously reported, cemento-enamel junction (CEJ) to alveolar bone crest (ABC) distance was significantly increased in S-LIP compared to NLC sites [8], but L-LIP resulted in an average of 70% ($p \leq 0.0014$) increase in the CEJ-ABC distance compared to S-LIP (Fig. 1A–B). Histologic analysis revealed increased inflammatory infiltrate and bone loss at the site of ligature placement that was accompanied by a 61% ($p=0.0325$) increase in osteoclast number in L-LIP compared to S-LIP groups (Fig. 1C–D, Supplemental Fig. 1D). No changes were observed in bone loss, osteoclast number, or histology between NLC sites in S-LIP and L-LIP, so all NLC samples were combined during analysis. Previous reports have

suggested that ligature placement elicits a systemic immune response that is both gender and time dependent [20,21], so we assessed pro-inflammatory cytokine expression in serum using a multiplex cytokine array. We observed an increase in cytokines such as IL1β, IL6, and IL17 in both LIP groups compared to the control, but differences were not significant (Supplemental Fig. 2). In contrast, chemokines PF4 and MIP1γ were significantly increased after ligature treatment compared to controls (Fig. 1E). Expression of pro-inflammatory cytokines in the liver and spleen was not dependent on LIP, whereas in the gingiva, *Il17a* expression was significantly increased by and average of 26-fold and 10-fold in L-LIP animals compared to S-LIP and NLC groups, respectively (Fig 1F, Supplemental Fig. 1E–G). Together, this proof-of-concept animal model establishes a clear difference in bone loss and cyto-/chemokine expression in S- and L-LIP.

Host response drives pathologic bone loss in L-LIP

In the LIP mouse model, the ligature supports microbe aggregation at the dentogingival junction which enables microbe invasion into the connective tissue [22]. Given the significant differences in pathologies between S-LIP and L-LIP, we aimed to understand whether this was due to altered microbe composition on the ligature or an extended host response to inflammation. 16S sequencing revealed significantly reduced alpha and beta diversity at the amplicon sequence variant level on S- and L-LIP ligatures compared to controls, but no differences were seen in diversity metrics between S-LIP and L-LIP alone (Fig. 2A–C), suggesting that there are no differences between the diversity of microbes on LIP ligatures after 3 or 10 weeks. To understand how differences in the length of ligature placement affect local immune responses, we stained coronal sections at the site of ligature placement with surface markers for T cells, tissue resident macrophages and granulocytes (Fig. 2D, Supplemental Fig. 3). Both CD3+ T cells and F4/80+ macrophages significantly increased in a time dependent manner, whereas CD66b+ granulocytes increased in S-LIP but not in L-LIP (Fig. 2E). The total number of immune cells per treatment condition were tallied to reveal that CD3+ T cells were the dominant stained cell in both health and disease (Fig. 2F). These data suggest that host response rather than microbiota composition is primarily responsible for pathologic bone loss associated with LIP.

Combined L-LIP and ZOL treatment induces osteonecrosis in mice

Although clinical BRONJ typically occurs after a tooth extraction or dental surgery, several animal studies have suggested that osteonecrosis develops in the presence of periodontal disease without tooth extraction [9,23]. To determine the effect of concomitant L-LIP and ZOL treatment on bone resorption and osteonecrosis development we treated a cohort of mice with combinations of L-LIP and/or ZOL (Fig. 3A). Examination of maxillae after 10 weeks revealed significant epithelial recession at vehicle (Veh) treated LIP sites that was not present in ZOL treated LIP or NLC sites (Supplemental Fig. 4A, **left**). μCT analysis showed a marked reduction in the palatal extent of bone resorption at L-LIP/ZOL sites compared to L-LIP/Veh sites (Supplemental Fig. 4A, **right, black arrowheads**). Sagittal views of μCT reconstructions demonstrated the efficacy of ZOL at completely inhibiting L-LIP-induced alveolar bone resorption (Fig 3B,C). Although we observed no significant difference in bone loss between L-LIP/ZOL and NLC animals, the bone surrounding the ligature site had a unique appearance compared to NLC sites such as intact ABC with roughened bone surface

that is broadly distributed underneath (Fig 3B, **white arrowheads**). Histologic analysis confirmed that the buccal bone directly adjacent to the ligature site was necrotic, and necrosis was only seen in the L-LIP/ZOL cohort (Fig 3D, E). L-LIP treatment resulted in a significant increase in the number of $TRAP^+$ osteoclasts regardless of antiresorptive therapy (Fig 3F, G). This data cumulatively suggests that osteonecrosis develops independently of tooth extractions in mice following L-LIP treatment.

Combined L-LIP and ZOL treatment followed by tooth extraction further exacerbates osteonecrosis development in mice

In our non-extraction L-LIP/ZOL mouse model we observed significant osteonecrosis development in the L-LIP/ZOL group but none in the NLC/ZOL group (Fig 3D–E). To isolate the role of tooth extraction and L-LIP in osteonecrosis pathogenesis, we observed bone phenotypes in mice treated with ZOL and/or L-LIP, where the ligatured tooth was extracted and underwent healing for 3 weeks (Fig. 4A). Photographs and μCT showed significant inhibition of extraction socket resorption in ZOL treated animals (Supplemental Fig. 5). Like L-LIP/ZOL animals without extraction, L-LIP/ZOL with extraction resulted in roughened bone surface visible by μCT, which was shown to be necrotic bone by histology (Fig. 4B, **white arrows**, C–D). In line with previous findings [7,8] we observed moderate osteonecrosis development in NLC/ZOL mice. Consequently, L-LIP/ZOL mice developed an average of 178% (p=0.0397) more osteonecrosis than NLC/ZOL mice (Fig. 4C–D). The number of $TRAP^+$ osteoclasts increased in all groups compared to the control, and the number of $TRAP^+$ osteoclasts was increased by 150% (p=0.0009) in L-LIP/ZOL compared to NLC/ZOL groups (Fig. 4E–F). Cumulatively, this data shows the additive effect of ligature-induced inflammation and tooth extraction on osteonecrosis development in mice.

Duration of ligature placement is associated with osteonecrosis development in mice

Previous studies have universally identified periodontitis as an important risk factor for the development of osteonecrotic lesions in rat models and in clinical studies. To determine whether the duration of ligature placement influences osteonecrosis development in mice, we assessed osteonecrosis development in L-LIP/ZOL and S-LIP/ZOL models (Supplemental Fig. 6A). Although gross photographs showed similar patterns of epithelial closure between L-LIP and S-LIP groups (Fig 5A, **black arrows**), μCT analysis confirmed that the bony sequestrum seen in previous L-LIP/ZOL studies was unique to the L-LIP group (Fig 5A, **white arrow**). Histologic analysis revealed that empty lacunae and percent bone necrosis increased by an average of 88% (p=0.0374) and 114% (p=0.0457), respectively, in L- compared to S-LIP mice (Fig 5B–C). Similarly, serum levels of MIP-1γ and PF4 increased in a time-dependent manner (Fig 5D). We previously found that CD3+ T cell counts increased following LIP in a time-dependent manner (Fig. 2D–F). “Type 17” cells are a subset of $CD3^+$ T cells that ubiquitously express IL23R [24], have been shown to drive the pathologic bone loss in periodontal disease [25] and have been implicated in a multiple myeloma model of BRONJ [26]. We quantified $CD3^+IL23R^+$ cells at the site of extraction and found significantly increased numbers in both S-LIP and L-LIP/ZOL samples compared to Veh controls. Additionally, there were an average of 116% (p=0.0402) more $CD3^+IL23R^+$ cells in L-LIP/ZOL cohorts compared to S-LIP/ZOL cohorts (Fig. 5E–F).

Together, these findings suggest that duration of periodontal inflammation is critical in osteonecrosis development and type 17 T cell recruitment.

DISCUSSION

In this study, we identify phenotypic characteristics of S-LIP and L-LIP mouse models for osteonecrosis development including differences in alveolar bone loss, osteoclast number, local and systemic expression of pro-inflammatory cytokines, microbiome, and local immune cell populations (Fig. 1, 2). We show that osteonecrosis develops in the L-LIP model combined with ZOL treatment in the absence of tooth extractions (Fig. 3, 4, 5G). Additionally, we show that the duration of local periodontitis inflammation is an important factor that significantly potentiates osteonecrosis development following tooth extraction, potentially due to heightened Type 17 T cell recruitment (Fig. 5A–F, H).

Although many confounding variables including genetic background, anti-resorptive dose, age, and others are controlled in animal models of osteonecrosis development, only a small percentage of animals develop BRONJ-like lesions in the absence of inflammation [7,8]. It is therefore critical to develop models that consistently produce a BRONJ-like phenotype to delineate pathophysiological factors that are reproducible. By inducing long-term inflammation, we have developed a model where almost all animals consistently develop some level of osteonecrosis (Fig. 5). Moreover, our L-LIP treatment results in significant bone loss (Fig. 1B), to the point where tooth prognosis is severely compromised which closely mimics a clinical situation that would warrant extraction.

A cytokine array detected significantly increased levels of PF4 and MIP-1γ in S-LIP and L-LIP (Fig. 1E). PF4 is stored within platelet α-granules and is released upon inflammation-induced platelet activation [27]. A link between platelet activity and periodontitis has been established [28–30] and studies have shown increased soluble PF4 in gingival crevicular fluid and serum of patients with severe periodontitis [31,32], suggesting that PF4 may be a marker of advanced periodontal disease. Assessment of PF4 in our mouse model of L-LIP combined with ZOL therapy and tooth extraction revealed a time-dependent increase in PF4 levels (Fig. 5D), Given that PF4 is degraded by matrix metalloproteinase 9 (MMP9) [33], which is inhibited by bisphosphonates like ZOL [34], it is conceivable that increased PF4 may possibly be due to decreased MMP9-mediated degradation by ZOL. Unlike PF4, less is known about MIP-1γ/CCL9. MIP-1γ is a major chemokine expressed by stimulated osteoclasts that activates cytoplasmic motility and spreading and plays an important role in bone resorption [35]. MIP-1γ also increases in a time dependent manner (Fig. 5D), which may be the result of increased secretion by bisphosphonate-stimulated osteoclasts. Interestingly, pro-inflammatory cytokine levels showed no major differences between S-LIP and L-LIP animals (Supplemental Fig. 2), suggesting that these pro-inflammatory cytokines are not systemically produced in significant quantities in our mouse model. Collectively, we speculate that PF4 and/or MIP-1γ may be used to identify patients taking bisphosphonates that have advanced periodontal disease and are therefore at high risk for developing BRONJ, though further testing is required to verify this finding in humans taking bisphosphonates.

Maintenance of barrier integrity is critical for host survival, and this is especially important during periodontal infection and following dentoalveolar surgery. The role of the oral microbiota in BRONJ pathogenesis remains controversial, although a recent study identified that there were no apparent differences in the microbial populations of BRONJ patients compared to healthy controls [36]. In line with this notion, our recent study demonstrated that indigenous microbiota protects, rather than exacerbates, against osteonecrosis development by ZOL in mice [19], suggesting that oral microbiota is unlikely to play a role in initiating osteonecrosis development.

Patients who developed BRONJ have significantly reduced expression of genes that regulate immune and barrier function [36]. The dominating immune population in both health and periodontal disease are $CD3^+$ T cells [37,38] which is corroborated in our study by histologic findings (Fig. 2F). In patients with osteonecrosis of the femoral head, Th17 and IL17 were both increased, and IL17 has been associated with the extraction socket of BRONJ patients undergoing surgical debridement [26,39]. The number of $CD3^+IL23R^+$ T cells is significantly higher at the extraction site in S-LIP and L-LIP mice treated with ZOL compared to Veh controls and increases with longer ligature placement periods. Additionally, these type 17 cells appear to aggregate around pieces of necrotic bone (Fig. 5F). Moreover, the length of ligature placement did not alter the diversity of microbes that colonized the ligature (Fig. 2A–C), suggesting that host response to inflammation plays a larger role than microbiota composition in pathologic bone loss and osteonecrosis development in our mouse model. Overall, further studies are warranted to determine the exact role of type 17 T cells in osteonecrosis development.

The duration of bisphosphonate treatment is an additional risk factor for the development of BRONJ in humans [40]. In our study, we compared animals with 3 weeks of combined ZOL/LIP exposure to animals with 10 weeks of combined ZOL/LIP exposure and found that animals in the latter cohort developed more osteonecrosis (Fig. 5). Further comparative studies are needed to delineate whether long-term exposure to bisphosphonate or duration of periodontal disease is more important in the development of osteonecrosis.

In summary, we have established and characterized a mouse model of long-term ligature-induced inflammation that leads to the development of osteonecrosis in mice. We have identified that the duration of inflammation is associated with the amount of necrotic bone formation following tooth extraction in mice receiving ZOL infusions. We have also observed a significant Type 17 T cell population that is localized to areas of inflammation-induced osteonecrosis. Our study corroborates findings in both humans [14,41] and animal models [42–44] that have suggested a role for periodontal disease in the pathogenesis of BRONJ and provides further evidence to support clinical guidelines that prioritize the resolution of pathologic inflammatory conditions in high-dose ZOL users to reduce the likelihood of osteonecrosis development.

Supplementary Material

Refer to Web version on PubMed Central for supplementary material.

ACKNOWLEDGEMENTS

We thank the University of California, Los Angeles Translational Procurement Core Laboratory for expedited and cooperative services. We also thank the UCLA BSCRC for use of core microscope facilities. Additionally, we thank the UCLA Technology Center for Genomics and Bioinformatics for expedited sequencing service.

This study was supported in part by the grants from NIH/NIDCR DE025172 (DWW) and DE023348 (RHK), SCADA Henry M. Thornton Fellowship (DWW), ADA Foundation Dentsply Sirona Research Award (DWW) and UCLA School of Dentistry Dean's Faculty Research Seed grant (RHK). The authors declare no potential conflicts of interest.

REFERENCES

1. Compston JE, McClung MR, Leslie WD. Osteoporosis. Lancet. Jan 26 2019;393(10169):364–76. Epub 2019/01/31. [PubMed: 30696576]
2. Neville-Webbe HL, Coleman RE. Bisphosphonates and RANK ligand inhibitors for the treatment and prevention of metastatic bone disease. Eur J Cancer. May 2010;46(7):1211–22. Epub 2010/03/30. [PubMed: 20347292]
3. Roelofs AJ, Thompson K, Gordon S, Rogers MJ. Molecular mechanisms of action of bisphosphonates: current status. Clinical cancer research : an official journal of the American Association for Cancer Research. Oct 15 2006;12(20 Pt 2):6222s–30s. Epub 2006/10/26. [PubMed: 17062705]
4. Kennel KA, Drake MT. Adverse effects of bisphosphonates: implications for osteoporosis management. Mayo Clin Proc. Jul 2009;84(7):632–7; quiz 8. Epub 2009/07/02. [PubMed: 19567717]
5. Marx RE. Pamidronate (Aredia) and zoledronate (Zometa) induced avascular necrosis of the jaws: a growing epidemic. Journal of oral and maxillofacial surgery : official journal of the American Association of Oral and Maxillofacial Surgeons. Sep 2003;61(9):1115–7. Epub 2003/09/11.
6. Aghaloo T, Hazboun R, Tetradis S. Pathophysiology of Osteonecrosis of the Jaws. Oral Maxillofac Surg Clin North Am. Nov 2015;27(4):489–96. Epub 2015/09/29. [PubMed: 26412796]
7. Williams DW, Lee C, Kim T, Yagita H, Wu H, Park S, et al. Impaired bone resorption and woven bone formation are associated with development of osteonecrosis of the jaw-like lesions by bisphosphonate and anti-receptor activator of NF-kappaB ligand antibody in mice. Am J Pathol. Nov 2014;184(11):3084–93. Epub 2014/09/01. [PubMed: 25173134]
8. Kim T, Kim S, Song M, Lee C, Yagita H, Williams DW, et al. Removal of Pre-Existing Periodontal Inflammatory Condition before Tooth Extraction Ameliorates Medication-Related Osteonecrosis of the Jaw-Like Lesion in Mice. Am J Pathol. Oct 2018;188(10):2318–27. Epub 2018/07/31. [PubMed: 30059656]
9. Aghaloo TL, Kang B, Sung EC, Shoff M, Ronconi M, Gotcher JE, et al. Periodontal disease and bisphosphonates induce osteonecrosis of the jaws in the rat. Journal of bone and mineral research : the official journal of the American Society for Bone and Mineral Research. Aug 2011;26(8):1871–82. Epub 2011/02/26.
10. Lescaille G, Coudert AE, Baaroun V, Ostertag A, Charpentier E, Javelot MJ, et al. Clinical study evaluating the effect of bevacizumab on the severity of zoledronic acid-related osteonecrosis of the jaw in cancer patients. Bone. Jan 2014;58:103–7. Epub 2013/10/15. [PubMed: 24120382]
11. Kim RH, Lee RS, Williams D, Bae S, Woo J, Lieberman M, et al. Bisphosphonates induce senescence in normal human oral keratinocytes. Journal of dental research. Jun 2011;90(6):810–6. Epub 2011/03/24. [PubMed: 21427353]
12. Kikuiri T, Kim I, Yamaza T, Akiyama K, Zhang Q, Li Y, et al. Cell-based immunotherapy with mesenchymal stem cells cures bisphosphonate-related osteonecrosis of the jaw-like disease in mice. Journal of bone and mineral research : the official journal of the American Society for Bone and Mineral Research. Jul 2010;25(7):1668–79. Epub 2010/03/05.
13. Thumbigere-Math V, Michalowicz BS, Hodges JS, Tsai ML, Swenson KK, Rockwell L, et al. Periodontal disease as a risk factor for bisphosphonate-related osteonecrosis of the jaw. Journal of periodontology. Feb 2014;85(2):226–33. Epub 2013/06/22. [PubMed: 23786404]

14. Khan AA, Morrison A, Kendler DL, Rizzoli R, Hanley DA, Felsenberg D, et al. Case-Based Review of Osteonecrosis of the Jaw (ONJ) and Application of the International Recommendations for Management From the International Task Force on ONJ. J Clin Densitom. Jan - Mar 2017;20(1):8–24. Epub 2016/12/14. [PubMed: 27956123]
15. Soundia A, Hadaya D, Esfandi N, Gkouveris I, Christensen R, Dry SM, et al. Zoledronate Impairs Socket Healing after Extraction of Teeth with Experimental Periodontitis. Journal of dental research. Mar 2018;97(3):312–20. Epub 2017/09/28. [PubMed: 28954199]
16. Song M, Alshaikh A, Kim T, Kim S, Dang M, Mehrazarin S, et al. Preexisting Periapical Inflammatory Condition Exacerbates Tooth Extraction-induced Bisphosphonate-related Osteonecrosis of the Jaw Lesions in Mice. Journal of endodontics. Nov 2016;42(11):1641–6. Epub 2016/10/30. [PubMed: 27637460]
17. Suh JS, Kim S, Bostrom KI, Wang CY, Kim RH, Park NH. Periodontitis-induced systemic inflammation exacerbates atherosclerosis partly via endothelial-mesenchymal transition in mice. Int J Oral Sci. Jul 1 2019;11(3):21. Epub 2019/07/02. [PubMed: 31257363]
18. Nair AB, Jacob S. A simple practice guide for dose conversion between animals and human. J Basic Clin Pharm. Mar 2016;7(2):27–31. Epub 2016/04/09. [PubMed: 27057123]
19. Williams DW, Vuong HE, Kim S, Lenon A, Ho K, Hsiao EY, et al. Indigenous Microbiota Protects against Inflammation-Induced Osteonecrosis. Journal of dental research. Jun 2020;99(6):676–84. Epub 2020/02/29. [PubMed: 32109361]
20. Bain JL, Lester SR, Henry WD, Bishop CM, Turnage AA, Naftel JP, et al. Comparative gender differences in local and systemic concentrations of pro-inflammatory cytokines in rats with experimental periodontitis. J Periodontal Res. Feb 2009;44(1):133–40. Epub 2009/06/12. [PubMed: 19515023]
21. Saadi-Thiers K, Huck O, Simonis P, Tilly P, Fabre JE, Tenenbaum H, et al. Periodontal and systemic responses in various mice models of experimental periodontitis: respective roles of inflammation duration and Porphyromonas gingivalis infection. Journal of periodontology. Mar 2013;84(3):396–406. Epub 2012/06/05. [PubMed: 22655910]
22. Graves DT, Kang J, Andriankaja O, Wada K, Rossa C Jr., Animal models to study host-bacteria interactions involved in periodontitis. Front Oral Biol. 2012;15:117–32. Epub 2011/12/07. [PubMed: 22142960]
23. Li CL, Lu WW, Seneviratne CJ, Leung WK, Zwahlen RA, Zheng LW. Role of periodontal disease in bisphosphonate-related osteonecrosis of the jaws in ovariectomized rats. Clinical oral implants research. Jan 2016;27(1):1–6. Epub 2014/11/06. [PubMed: 25371026]
24. Cua DJ, Tato CM. Innate IL-17-producing cells: the sentinels of the immune system. Nature reviews Immunology. Jul 2010;10(7):479–89. Epub 2010/06/19.
25. Dutzan N, Kajikawa T, Abusleme L, Greenwell-Wild T, Zuazo CE, Ikeuchi T, et al. A dysbiotic microbiome triggers TH17 cells to mediate oral mucosal immunopathology in mice and humans. Sci Transl Med. Oct 17 2018;10(463). Epub 2018/10/20.
26. Zhang Q, Atsuta I, Liu S, Chen C, Shi S, Shi S, et al. IL-17-mediated M1/M2 macrophage alteration contributes to pathogenesis of bisphosphonate-related osteonecrosis of the jaws. Clinical cancer research : an official journal of the American Association for Cancer Research. Jun 15 2013;19(12):3176–88. Epub 2013/04/26. [PubMed: 23616636]
27. Harrison P, Cramer EM. Platelet alpha-granules. Blood Rev. Mar 1993;7(1):52–62. Epub 1993/03/01.
28. Papapanagiotou D, Nicu EA, Bizzarro S, Gerdes VE, Meijers JC, Nieuwland R, et al. Periodontitis is associated with platelet activation. Atherosclerosis. Feb 2009;202(2):605–11. Epub 2008/07/12. [PubMed: 18617175]
29. Nicu EA, Van der Velden U, Nieuwland R, Everts V, Loos BG. Elevated platelet and leukocyte response to oral bacteria in periodontitis. J Thromb Haemost. Jan 2009;7(1):162–70. Epub 2008/11/06. [PubMed: 18983491]
30. Al-Rasheed A Elevation of white blood cells and platelet counts in patients having chronic periodontitis. Saudi Dent J. Jan 2012;24(1):17–21. Epub 2012/01/01. [PubMed: 23960523]

31. Greinacher A, Holtfreter B, Krauel K, Gatke D, Weber C, Ittermann T, et al. Association of natural anti-platelet factor 4/heparin antibodies with periodontal disease. Blood. Aug 4 2011;118(5):1395–401. Epub 2011/06/11. [PubMed: 21659541]
32. Brousseau-Nault M, Kizhakkedathu JN, Kim H. Chronic periodontitis is associated with platelet factor 4 (PF4) secretion: A pilot study. J Clin Periodontol. Nov 2017;44(11):1101–11. Epub 2017/07/07. [PubMed: 28681377]
33. Van den Steen PE, Proost P, Wuyts A, Van Damme J, Opdenakker G. Neutrophil gelatinase B potentiates interleukin-8 tenfold by aminoterminal processing, whereas it degrades CTAP-III, PF-4, and GRO-alpha and leaves RANTES and MCP-2 intact. Blood. Oct 15 2000;96(8):2673–81. Epub 2000/10/07. [PubMed: 11023497]
34. Teronen O, Heikkila P, Konttinen YT, Laitinen M, Salo T, Hanemaaijer R, et al. MMP inhibition and downregulation by bisphosphonates. Annals of the New York Academy of Sciences. Jun 30 1999;878:453–65. Epub 1999/07/23. [PubMed: 10415748]
35. Lean JM, Murphy C, Fuller K, Chambers TJ. CCL9/MIP-1gamma and its receptor CCR1 are the major chemokine ligand/receptor species expressed by osteoclasts. J Cell Biochem. 2002;87(4):386–93. Epub 2002/10/25. [PubMed: 12397598]
36. Kalyan S, Wang J, Quabius ES, Huck J, Wiltfang J, Baines JF, et al. Systemic immunity shapes the oral microbiome and susceptibility to bisphosphonate-associated osteonecrosis of the jaw. J Transl Med. Jul 4 2015;13:212. Epub 2015/07/05. [PubMed: 26141514]
37. Dutzan N, Konkel JE, Greenwell-Wild T, Moutsopoulos NM. Characterization of the human immune cell network at the gingival barrier. Mucosal immunology. Sep 2016;9(5):1163–72. Epub 2016/01/07. [PubMed: 26732676]
38. Williams DW, Greenwell-Wild T, Brenchley L, Dutzan N, Overmiller A, Sawaya AP, et al. Human oral mucosa cell atlas reveals a stromal-neutrophil axis regulating tissue immunity. Cell. Jun 9 2021. Epub 2021/06/16.
39. Zou D, Zhang K, Yang Y, Ren Y, Zhang L, Xiao X, et al. Th17 and IL-17 exhibit higher levels in osteonecrosis of the femoral head and have a positive correlation with severity of pain. Endokrynol Pol. 2018;69(3):283–90. Epub 2018/06/29. [PubMed: 29952419]
40. Ruggiero SL. Guidelines for the diagnosis of bisphosphonate-related osteonecrosis of the jaw (BRONJ). Clin Cases Miner Bone Metab. Jan 2007;4(1):37–42. Epub 2007/01/01. [PubMed: 22460751]
41. Hellstein JW, Adler RA, Edwards B, Jacobsen PL, Kalmar JR, Koka S, et al. Managing the care of patients receiving antiresorptive therapy for prevention and treatment of osteoporosis: executive summary of recommendations from the American Dental Association Council on Scientific Affairs. Journal of the American Dental Association. Nov 2011;142(11):1243–51. [PubMed: 22041409]
42. Messer JG, Mendieta Calle JL, Jiron JM, Castillo EJ, Van Poznak C, Bhattacharyya N, et al. Zoledronic acid increases the prevalence of medication-related osteonecrosis of the jaw in a dose dependent manner in rice rats (Oryzomys palustris) with localized periodontitis. Bone. Mar 2018;108:79–88. Epub 2018/01/01. [PubMed: 29289789]
43. Messer JG, Jiron JM, Mendieta Calle JL, Castillo EJ, Israel R, Phillips EG, et al. Zoledronate treatment duration is linked to bisphosphonate-related osteonecrosis of the jaw prevalence in rice rats with generalized periodontitis. Oral diseases. May 2019;25(4):1116–35. Epub 2019/02/04. [PubMed: 30712276]
44. Aguirre JI, Akhter MP, Kimmel DB, Pingel JE, Williams A, Jorgensen M, et al. Oncologic doses of zoledronic acid induce osteonecrosis of the jaw-like lesions in rice rats (Oryzomys palustris) with periodontitis. Journal of bone and mineral research : the official journal of the American Society for Bone and Mineral Research. Oct 2012;27(10):2130–43. Epub 2012/05/25.

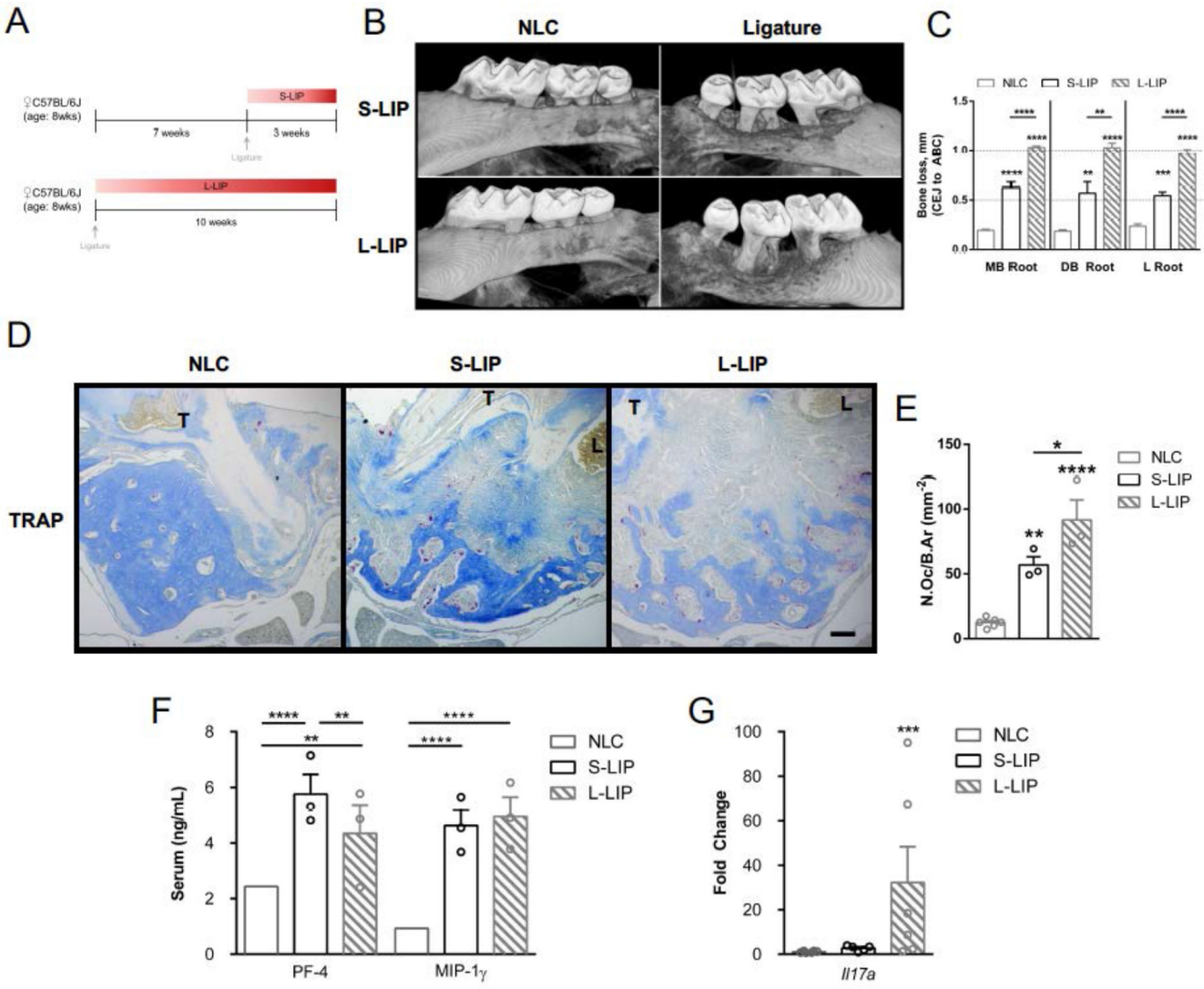

Figure 1.

Phenotypic characterization of short- and long-term ligature induced periodontitis. A. Visual representation of the experimental timeline. Briefly, 8-week-old C57BL/6J mice were split into two groups. The first group received no treatment for 7 weeks, and then a 6-0 silk suture was tied around the second maxillary molar. The second group received the suture for 10 weeks. B. Saggital view of μCT scanned and reconstructed maxilla depicting buccal bone loss at ligature and no-ligature control sites in S-LIP and L-LIP mice. No differences were seen between NLC from S-LIP and L-LIP samples, so these sites were combined into a single 'NLC' group for analysis. C. Quantification of bone loss at each of the second maxillary molar roots. D. TRAP staining on coronal histologic sections at the site of ligation. Tooth (T) and ligature (L) are labeled for reference. Bar: 100μm. E. Quantification of TRAP-positive multinucleated osteoclasts at the site of ligature placement. F. Serum analysis of pro-inflammatory cytokine array targets platelet factor 4 (PF-4) and macrophage inflammatory factor 1 gamma (MIP-1γ). G. Quantitative real-time PCR of gingival tissue taken from ligature or no-ligature control sites. S-LIP, short-term ligature-

induced periodontitis (3 weeks); L-LIP, long-term ligature-induced periodontitis (10 weeks), NLC, no-ligature control; MB, mesio-buccal; DB, disto-buccal; L (root), lingual; N.Oc/B.Ar, number of osteoclasts per bone area. *p<0.05; **p<0.01; ***p<0.001; ****p<0.0001. Data is presented as mean ± SEM.

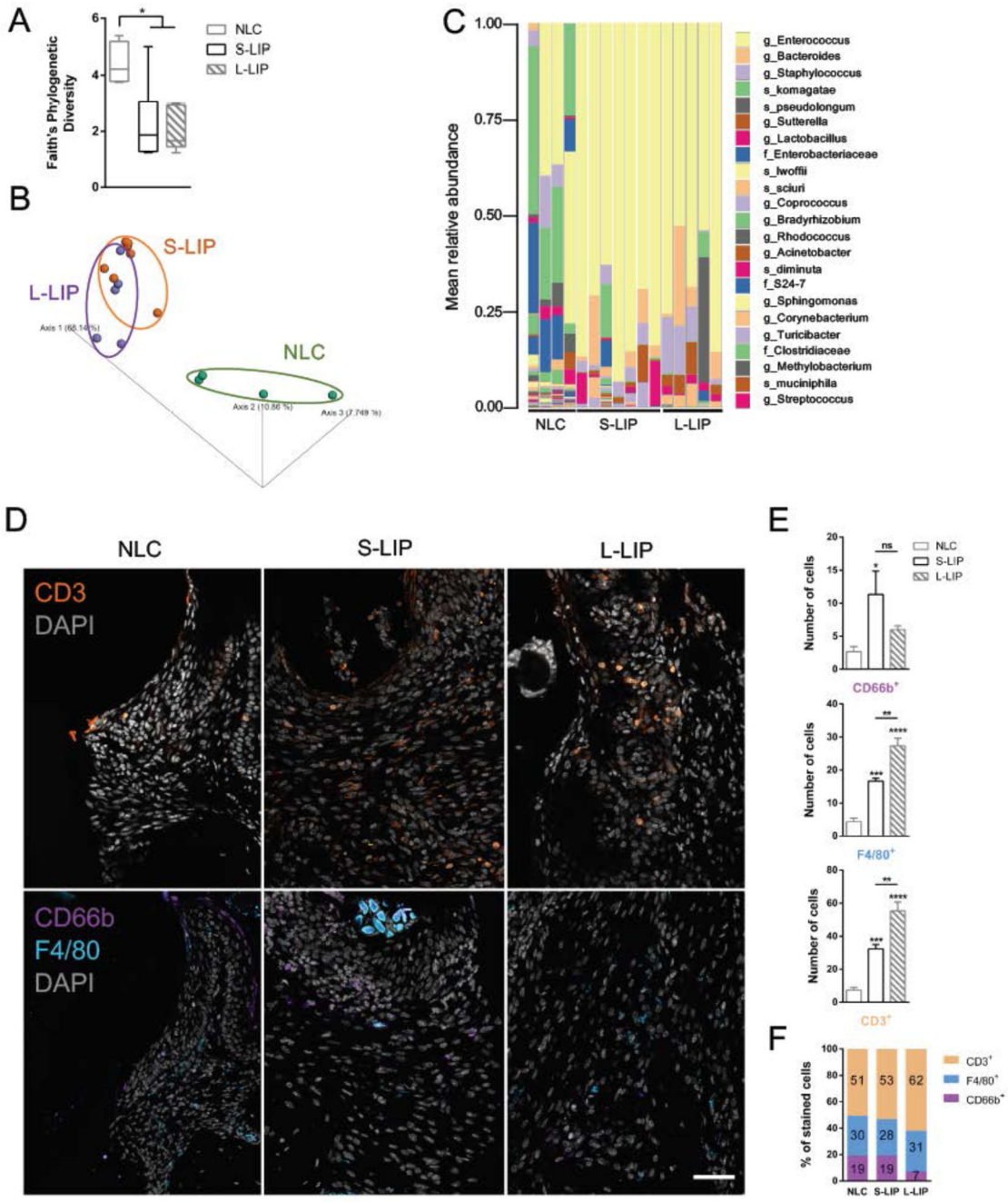

Figure 2.

Host response drives pathologic bone loss in LIP. A,B. The alpha (A) and beta (B) diversity of the microbial communities found at the site of ligature placement were calculated by Faith's phylogenetic diversity and Bray-Curtis dissimilarity principal component analysis, respectively. C. Microbiome composition is shown at the amplicon sequence variant level (ASV). The top 23 ASVs are classified at the highest taxonomic level identified. s_, species; g_, genus; f_, family. D-F. Representative images and quantification of immunofluorescent staining at the site of ligature placement. The number of stained cells (E) were counted and

the proportion of each cell type present was tallied (F). Scale bar: 50μm. S-LIP, short-term ligature-induced periodontitis (3 weeks); L-LIP, long-term ligature-induced periodontitis (10 weeks), NLC, no-ligature control; *p<0.05; **p<0.01; ***p<0.001; ****p<0.0001. Data is presented as mean ± SEM.

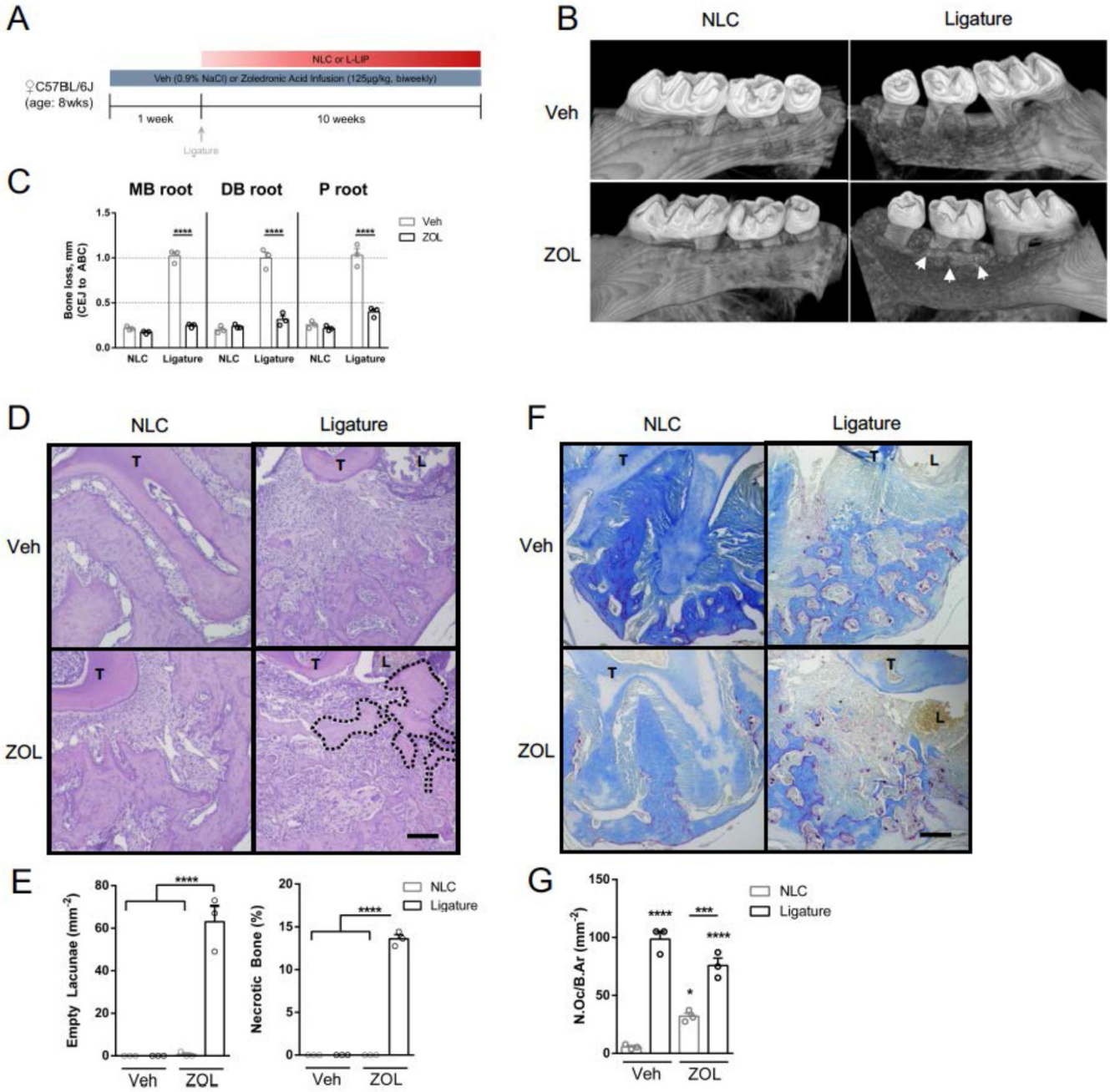

Figure 3.

Long-term ligature and anti-resorptive therapy leads to extraction-independent osteonecrosis. A. 8-week-old C57BL/6 mice were split into two groups. These groups received biweekly intravenous injections of vehicle or zoledronic acid for the entire study. After one week of infusions, half of the mice in each group received a suture as described in Figure 1A for 10 weeks. B. Sagittal view of μCT scanned and reconstructed maxilla depicting buccal bone loss. White arrowheads point to necrotic bone at the site of ligature placement visible by μCT. C. Quantification of bone loss at each of the second maxillary molar roots. D. Hematoxylin & Eosin staining on coronal histologic sections at the site of

ligation. Tooth (T) and ligature (L) are labeled for reference. Necrotic bone is outlined by the black dotted line. Scale bar: 100μm. E. Quantification of empty lacunae (left) and necrotic bone (right) from histology sections. F. TRAP staining on coronal histologic sections at the site of ligation. Tooth (T) and ligature (L) are labeled for reference. Scale bar: 100μm. G. Quantification of TRAP-positive multinucleated osteoclasts at the site of ligature placement. Veh, vehicle; ZOL, zoledronic acid; NLC, no-ligature control; MB, mesio-buccal; DB, disto-buccal; P, palatal; N.Oc/B.Ar, number of osteoclasts per bone area. *$p<0.05$; **$p<0.01$; ***$p<0.001$; ****$p<0.0001$. Data is presented as mean ± SEM.

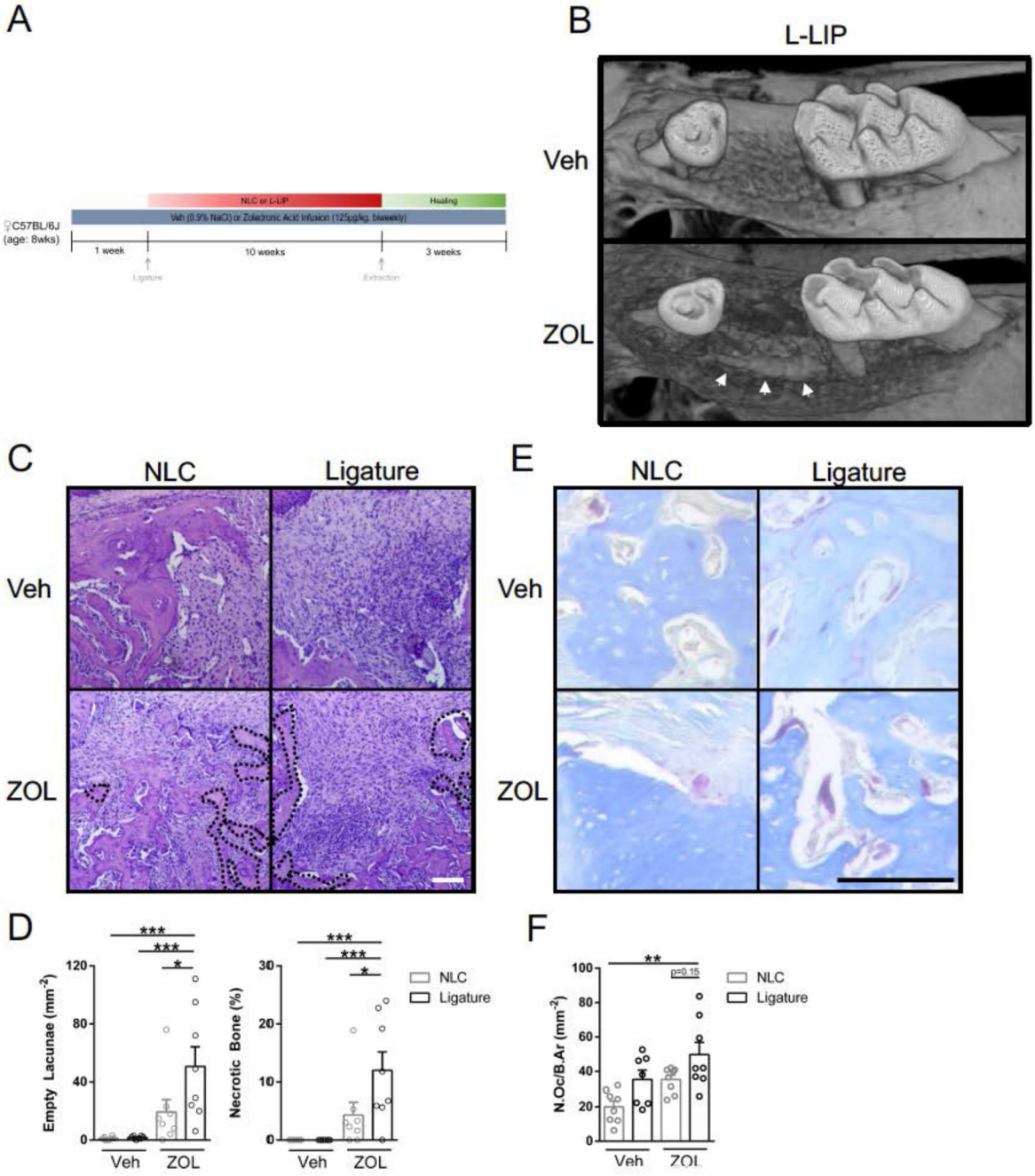

Figure 4.

Long-term ligature and anti-resorptive therapy leads to post-extraction osteonecrosis. A. Mice were divided exactly as in Figure 3A. After 10 weeks of ligature, mice underwent bilateral second maxillary molar extractions and were allowed to heal for 3 weeks prior to sacrifice. B. μCT reconstructed photographs depicting extent of socket remodeling. White arrowheads point to necrotic bone at the second maxillary molar visible by μCT. B. Hematoxylin & Eosin staining on coronal histologic sections at the extraction site. Necrotic bone is outlined by the black dotted lines. Scale bar: 100μm. C. Quantification of

empty lacunae (left) and necrotic bone (right) from histology sections. D. TRAP staining on coronal histologic sections at the site of extraction. Scale bar: 100μm. E. Quantification of TRAP-positive multinucleated osteoclasts at the site of extraction. Veh, vehicle; ZOL, zoledronic acid; NLC, no-ligature control; N.Oc/B.Ar, number of osteoclasts per bone area. *$p<0.05$; **$p<0.01$; ***$p<0.001$. Data is presented as mean ± SEM.

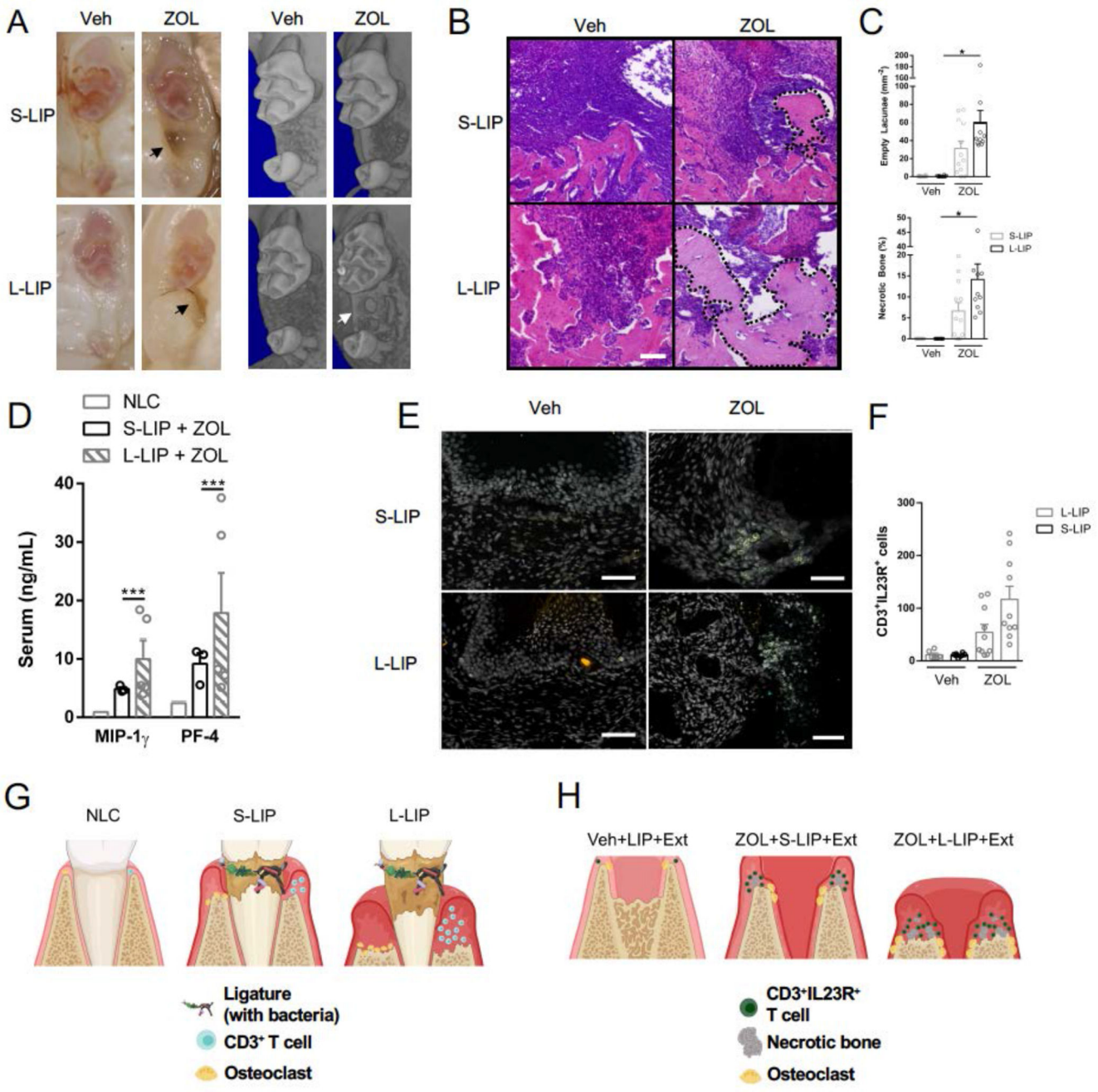

Figure 5.

Osteonecrosis development is dependent on duration of ligature-induced periodontitis. A. Clinical (left) and μCT (right) reconstructed photographs depicting epithelial and osseous healing following extraction. Black arrowheads show exposed bone with incomplete epithelial closure. White arrowhead points to necrotic bone at the site of extraction visible by μCT. B. Hematoxylin & Eosin staining on coronal histologic sections at the site of tooth extraction. Necrotic bone is outlined by the black dotted lines. Scale bar: 100μm. C. Quantification of empty lacunae (top) and necrotic bone (bottom) from histology sections.

D. Serum analysis of pro-inflammatory cytokine array targets platelet factor 4 (PF-4) and macrophage inflammatory factor 1 gamma (MIP-1γ). E,F. Representative images and quantification of dual labeled immunofluorescent staining colocalized to DAPI at the site of extraction. Scale bar: 50μm. G,H. Summary illustration of findings. (G) In L-LIP, the number of osteoclasts and $CD3^+$ T cells is increased compared to S-LIP, but the number and type of bacteria is the same. (H) When LIP is combined with antiresorptive therapy and extraction, the amount of necrotic bone and number of $CD3^+IL23R^+$ T cells is increased in L-LIP compared to S-LIP. Cartoons made with Biorender.com. Veh, vehicle; ZOL, zoledronic acid; S-LIP, short-term ligature-induced periodontitis; L-LIP, long-term ligature-induced periodontitis. *$p<0.05$; ***$p<0.001$. Data is presented as mean ± SEM.